

Electronic Supplementary Information (ESI)

Co-Cu-WS_x ball-in-ball nanosphere as high-performance Pt-free bifunctional catalyst in efficient dye-sensitized solar cell and alkaline hydrogen evolution

Xing Qian,* Hongyu Liu, Jiahui Yang, Huiwen Wang, Jie Huang and Chong Xu

College of Chemical Engineering, Fuzhou University, Xueyuan Road No. 2, Fuzhou 350116, China. E-mail: xinqian@fzu.edu.cn. Fax: +86-0591-2286 6244; Tel: +86-0591-2286 5220.

Materials

Cobalt nitrate hexahydrate ($\text{Co}(\text{NO}_3)_2 \cdot 6\text{H}_2\text{O}$, AR), copper (II) nitrate trihydrate ($\text{Cu}(\text{NO}_3)_2 \cdot 3\text{H}_2\text{O}$, AR), ammonium metatungstate hydrate ($(\text{NH}_4)_6\text{H}_2\text{W}_{12}\text{O}_{40} \cdot x\text{H}_2\text{O}$, AR) and thioacetamide (TAA, AR) were obtained from Aladdin Ltd. (China). Ammonium metatungstate hydrate was procured from Aladdin Ltd. Lithium iodide (LiI , ≥ 99.0%), iodine (I_2 , ≥ 99.9%), lithium perchlorate (LiClO_4 , ≥ 99.9%) were purchased from Macklin Ltd. (China). The commercial N719 dye and Pt/C (20 wt%) powder were received from Solaronix Ltd. (Switzerland). The fluorine-doped SnO_2 (FTO) glasses, purchased from Nippon Sheet Glass(15 Ω sq^{-1} , Japan), were cleaned with cleanser essence, acetone and ethyl alcohol in sequence and cut into squares of 1.5 cm × 1.5 cm.

Instruments

The surface morphologies of all samples were observed by a scanning electron microscopy (SEM, S-4800, Hitachi). Powder XRD patterns were carried out on X-ray diffraction (XRD, X'Pert PRO, Cu K α , $\lambda = 0.15406$ nm) for the indication of crystal structure. The microstructures of Co-Ni-MoS_x YSNs were investigated through a high-resolution transmission electron microscope (HRTEM, TECNAI, G2F20, FEI), equipped with an accessory of energy-dispersive X-ray spectroscopy (EDX). X-ray photoelectron spectroscopy (XPS) analysis was conducted on a VG ESCALAB 250 (Mg K α , USA) spectrometer to characterize the elemental composition of Co-

Ni-MoS_x YSNs. The surface area and pore-size distribution were measured by a Micromeritics ASAP-2020.

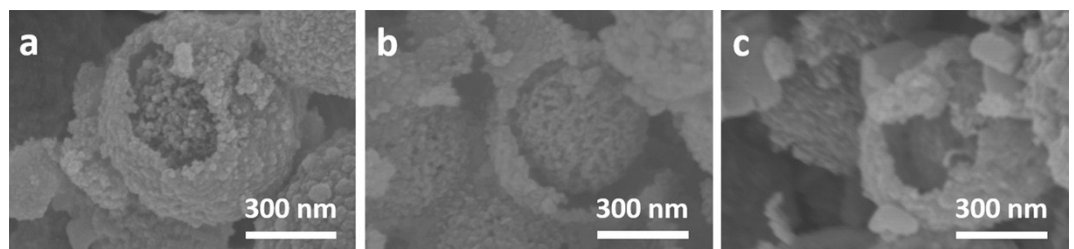


Fig. S1. SEM images of (a) cracked Co-Cu-WS_x, (b) cracked Co-WS_x, (c) cracked Co-CuS_x after the ultrasonic treatment

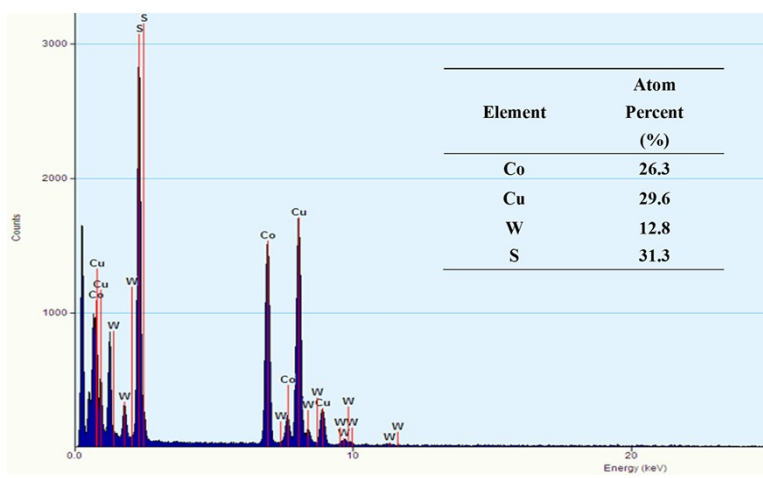


Fig. S2. EDX spectra images and main atom percent of Co-Cu-WS_x.

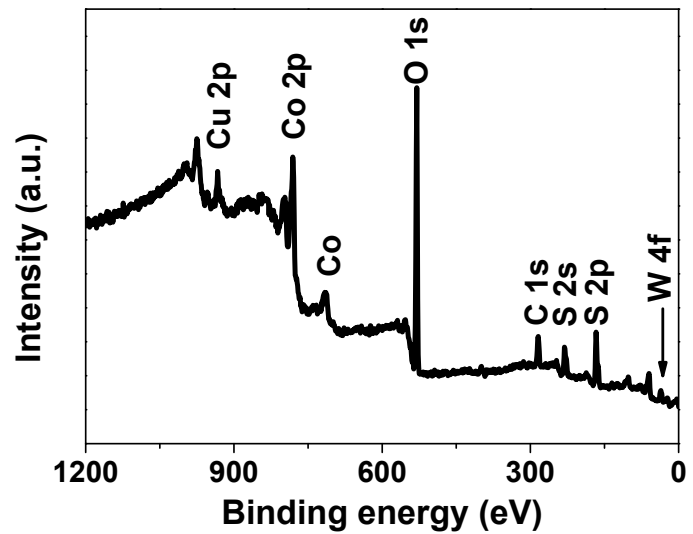


Fig. S3. XPS spectra of Co-Cu-WS_x survey spectrum.

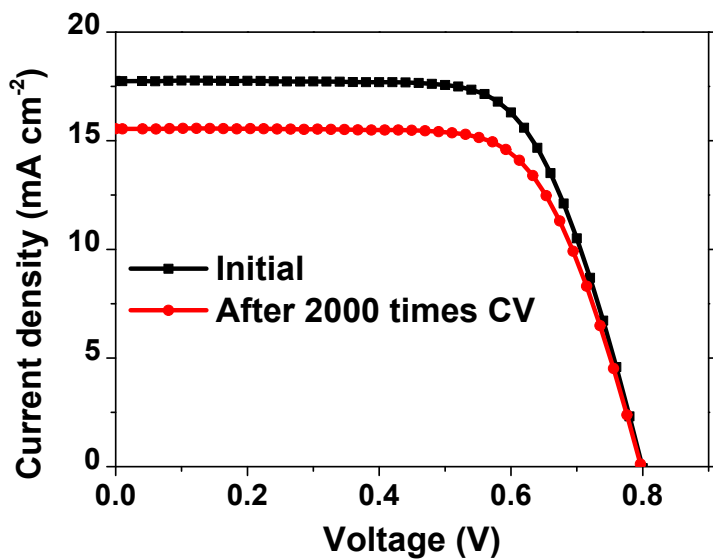


Fig. S4. J - V curves of Co-Cu-WS_x based CE before and after 2000 CV cycles.

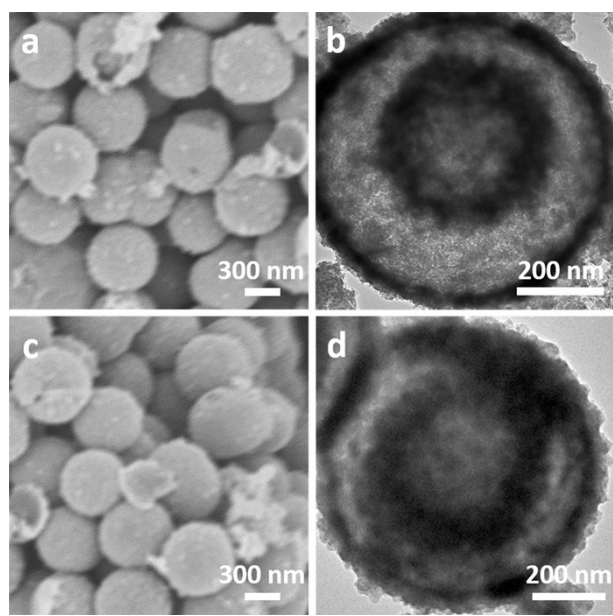


Fig. S5. (a, b) SEM/TEM images of Co-Cu-WS_x after stability tests for DSSC. (c, d) SEM/TEM images of Co-Cu-WS_x after stability tests for HER.

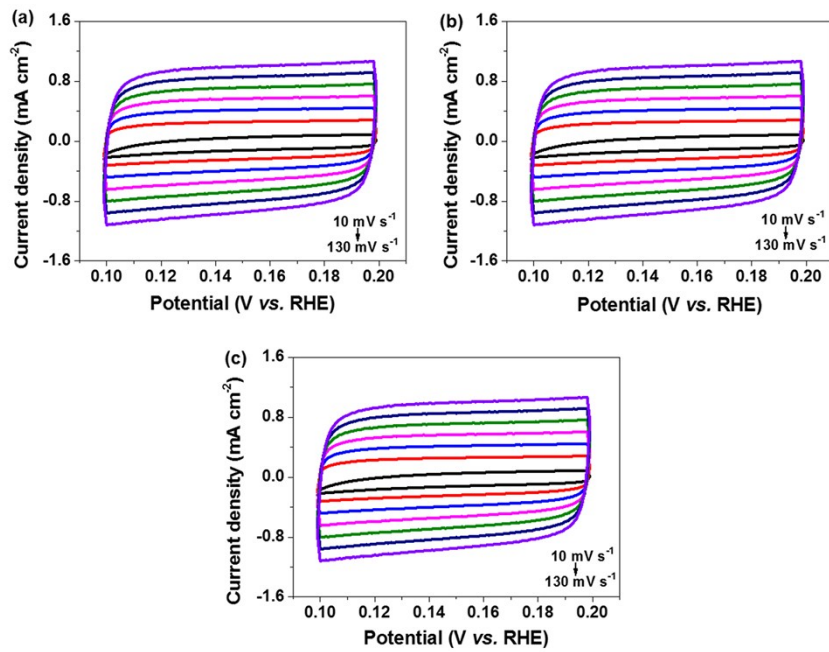


Figure S6. Cycle voltammograms of (a) Co-Cu-WS_x, (b) Co-WS_x and (c) Co-CuS_x at different scan rates (10, 30, 50, 70, 90, 110 and 130 mV s⁻¹) in 1.0 M KOH.

Table S1. Comparisons of DSSC performances for Co-Cu-WS_x with other typical non-noble metal-based catalysts.

Catalyst	η (%)	η_{Pt} (%)	η/η_{Pt}	Reference
Co-Cu-WS _x	9.61	8.24	1.17	This work
CuS/WS ₂	8.21	7.97	1.03	1
Co ₃ S ₄ nanosheet/rGO	8.08	7.62	1.06	2
WO _x @WS ₂ @carbon	7.71	7.34	1.05	3
Co ₃ S ₄ /ECs	9.23	8.38	1.10	4
MoS ₂ /Co ₃ S ₄	6.77	7.14	0.95	5
CoS on om-SnO ₂	7.50	5.80	1.29	6
carbon-coated WS ₂	5.50	5.60	0.98	7
WS ₂ /MWCNTa	7.36	7.54	0.98	8
WS ₂	7.73	7.64	1.01	9

Table S2. Comparison of HER performance in alkaline medium for as-obtained samples with other non-noble metal-based catalysts.

Catalyst	Onset potential (mV)	η_{10} (mV)	Tafel slope (mV decade $^{-1}$)	Reference
Co-Cu-WS _x	25.5	82.5	53.8	This work
Co ₃ S ₄ HNSs	—	221	111	10
Co ₃ S ₄ /MoS ₂ /Ni ₂ P	60	—	98	11
Co ₃ S ₄ @MoS ₂	—	136	74.	12
MoS ₂ /Co ₃ S ₄	—	225	115.3	13
γ -Cu ₂ S/CF	105	190	98.9	14
NiO@Ni/WS ₂ /CC	40	—	43	15
Co ₃ S ₄ /CoP	38	86	45	16
NiS ₂ /MoS ₂ HNW	—	204	65	17
WS ₂ /SNCF	96	157	66	18

References

- 1 S. Hussain, S. A. Patil, A. A. Memon, D. Vikraman, B. A. Naqvi, S. H. Jeong, H. S. Kim, H. S. Kim and J. Jung, *Sol. Energy*, 2018, **171**, 122–129.
- 2 T. T. Jiang, S. Y. Yang, P. Dai, X. X. Yu, Z. M. Bai, M. Z. Wu, G. Li and C. J. Tu, *Electrochim. Acta*, 2018, **261**, 143–150.
- 3 Z. F. Shen, M. W. Wang, L. H. Liu, M. V. Sofianos, H. G. Yang, S. B. Wang and S. M. Liu, *Electrochim. Acta*, 2018, **266**, 130–138.
- 4 L. Li, J. Y. Xiao, H. D. Sui, X. C. Yang, W. M. Zhang, X. W. Li, A. Hagfeldt and M. X. Wu, *J. Power Sources*, 2016, **326**, 6–13.
- 5 F. Y. Dong, Y. J. Guo, P. Xu, X. Yin, Y. G. Li and M. He, *Sci. China Mater.*, 2017, **60**, 295–303.
- 6 J. T. Park, C. S. Lee and J. H. Kim, *Nanoscale*, 2015, **7**, 670–678.
- 7 Y. Y. Wang, S. J. Li, Y. Bai, Z. Chen, Q. W. Jiang, T. Li and W. F. Zhang, *Electrochim. Acta*, 2013, **114**, 30–34.
- 8 J. Wu, G. Yue, Y. Xiao, M. Huang, J. Lin, L. Fan, Z. Lan and J. Y. Lin, *ACS Appl. Mater. Interfaces*, 2012, **4**, 6530–6536.
- 9 M. Wu, Y. Wang, X. Lin, N. Yu, L. Wang, L. Wang, A. Hagfeldt and T. Ma, *Phys. Chem. Chem. Phys.*, 2011, **13**, 19298–19301.
- 10 X. Ma, W. Zhang, Y. Deng, C. Zhong, W. Hu and X. Han, *Nanoscale*, 2018, **10**, 4816–4824.
- 11 H. Lin, H. Li, Y. Li, J. Liu, X. Wang and L. Wang, *J. Mater. Chem. A*, 2017, **5**, 25410–25419.
- 12 Y. N. Guo, J. Tang, Z. L. Wang, Y. M. Kang, Y. Bando and Y. Yamauchi, *Nano Energy*, 2018, **47**, 494–502.
- 13 X. Lei, K. Yu, H. L. Li and Z. Q. Zhu, *Electrochim. Acta*, 2018, **269**, 262–273.
- 14 M. H. Fan, R. Q. Gao, Y. C. Zou, D. J. Wang, N. Bai, G. D. Li and X. X. Zou, *Electrochim. Acta*, 2016, **215**, 366–373.
- 15 D. Wang, Q. Li, C. Han, Z. Xing and X. Yang, *ACS Cent. Sci.*, 2018, **4**, 112–119.
- 16 T. Wang, L. Wu, X. Xu, Y. Sun, Y. Wang, W. Zhong and Y. Du, *Sci. Rep.*, 2017, **7**,

11891.

- 17 P. Y. Kuang, T. Tong, K. Fan and J. G. Yu, *ACS Catal.*, 2017, **7**, 6179–6187.
18 Q. F. Wang, R. P. Yanzhang, X. N. Ren, H. Zhu, M. Zhang and M. L. Du, *Int. J. Hydrogen Energy*, 2016, **41**, 21870–21882.